JOURNAL OF GEOPHYSICAL RESEARCH, VOL. 113, C02017, doi:10.1029/2007JC004359, 2008

Decadal variability in the northeast Pacific in a physical-ecosystem model: Role of mixed layer depth and trophic interactions

Michael Alexander,[1] Antonietta Capotondi,[1] Arthur Miller,[2] Fei Chai,[3] Richard Brodeur,[4] and Clara Deser[5]

Received 25 May 2007; revised 13 September 2007; accepted 16 November 2007; published 21 February 2008.

[1] A basin-wide interdecadal change in both the physical state and the ecology of the North Pacific occurred near the end of 1976. Here we use a physical-ecosystem model to examine whether changes in the physical environment associated with the 1976–1977 transition influenced the lower trophic levels of the food web and if so by what means. The physical component is an ocean general circulation model, while the biological component contains 10 compartments: two phytoplankton, two zooplankton, two detritus pools, nitrate, ammonium, silicate, and carbon dioxide. The model is forced with observed atmospheric fields during 1960–1999. During spring, there is a ~40% reduction in plankton biomass in all four plankton groups during 1977–1988 relative to 1970–1976 in the central Gulf of Alaska (GOA). The epoch difference in plankton appears to be controlled by the mixed layer depth. Enhanced Ekman pumping after 1976 caused the halocline to shoal, and thus the mixed layer depth, which extends to the top of the halocline in late winter, did not penetrate as deep in the central GOA. As a result, more phytoplankton remained in the euphotic zone, and phytoplankton biomass began to increase earlier in the year after the 1976 transition. Zooplankton biomass also increased, but then grazing pressure led to a strong decrease in phytoplankton by April followed by a drop in zooplankton by May: Essentially, the mean seasonal cycle of plankton biomass was shifted earlier in the year. As the seasonal cycle progressed, the difference in plankton concentrations between epochs reversed sign again, leading to slightly greater zooplankton biomass during summer in the later epoch.

Citation: Alexander, M., A. Capotondi, A. Miller, F. Chai, R. Brodeur, and C. Deser (2008), Decadal variability in the northeast Pacific in a physical-ecosystem model: Role of mixed layer depth and trophic interactions, *J. Geophys. Res.*, *113*, C02017, doi:10.1029/2007JC004359.

1. Introduction

[2] Studies conducted over the past 15–20 years have provided a growing body of evidence for decadal climate variability across the Pacific Basin [e.g., *Trenberth*, 1990; *Graham*, 1994; *Zhang et al.*, 1997; *Deser et al.*, 2004]. The most prominent mode of decadal variability in the North Pacific was termed the Pacific Decadal Oscillation (PDO) by *Mantua et al.* [1997] on the basis of transitions between relatively stable states of the leading pattern of sea surface temperature (SST) anomalies. The 1976–1977 transition or "regime shift" was especially pronounced, with an increase in the strength of the atmospheric circulation over the North Pacific that resulted in basin-wide changes in ocean temperatures, currents, and mixed layer depth [e.g., *Miller et al.*, 1994; *Trenberth and Hurrell*, 1994; *Polovina et al.*, 1995; *Deser et al.*, 1996, 1999]. These climatic changes had a pervasive effect on marine ecosystems from phytoplankton to the top trophic levels [e.g., *Mantua et al.*, 1997; *Hare and Mantua*, 2000; *Benson and Trites*, 2002].

[3] While the dynamics underlying Pacific decadal variability have not been fully resolved, changes in the physical state of the ocean clearly influence the primary and secondary production in the North Pacific. For example, total chlorophyll *a*, a proxy for phytoplankton biomass, nearly doubled in the central North Pacific from 1968 to 1985 [*Venrick et al.*, 1987]. *Brodeur and Ware* [1992], *Brodeur et al.* [1996], and *Rand and Hinch* [1998] found that the zooplankton biomass in summer was relatively high in the central portion of the Gulf of Alaska (GOA) during 1956–1962, while in 1980–1989 the biomass was greatest along the edges of the Alaskan Gyre. Overall, the zooplankton biomass nearly doubled over the northeast Pacific in the 1980s relative to the late 1950s and early 1960s during

[1]Earth System Research Laboratory, NOAA, Boulder, Colorado, USA.
[2]Scripps Institution of Oceanography, University of California, San Diego, La Jolla, California, USA.
[3]School of Marine Sciences, University of Maine, Orono, Maine, USA.
[4]Northwest Fisheries Science Center, Hatfield Marine Science Center, Oregon State University, Newport, Oregon, USA.
[5]Climate and Global Dynamics Division, National Center for Atmospheric Research, Boulder, Colorado, USA.

0148-0227/08/2007JC004359$09.00

summer. *McFarlane and Beamish* [1992] also found that the copepod biomass increased after the winter of 1976–1977 in the Gulf of Alaska. In contrast, *Sugimoto and Tadokoro* [1997] found a decrease in both phytoplankton and zooplankton biomass in the northeast Pacific during the summers of 1980–1994 relative to those in 1960–1975. Some of the differences between these estimates of decadal variations may be due to the large interannual and spatial variability of zooplankton biomass, especially given the limited number of measurements.

[4] While the PDO provides an important means for linking variability over the North Pacific, climatic shifts appear to be more complex than just reversals between two nearly opposite states [*Benson and Trites*, 2002]. For example, *Bond et al.* [2003] examined the state of the North Pacific Ocean via the amplitudes of first and second leading patterns of SST variability as identified by empirical orthogonal function (EOF) analysis. While the years 1970–1976 and 1978–1988 were dominated by the opposite phases of the PDO (first EOF), its amplitude was relatively modest during most of the 1960s, and the 1989 transition was primarily from the first to the second EOF. On the basis of these findings, and following many previous studies, we will explore the climate transition in the northeast Pacific from the difference between 1970–1976 and 1977–1988. We will also examine the full 40-year record since Pacific climate and ecosystem indices do not always coincide with the PDO because of other patterns of variability, lags in the system, and/or a lack of sensitivity to PDO-related SST anomalies.

[5] Several physical/geochemical factors may influence primary productivity in the Pacific on interannual to decadal timescales, including temperature, sunlight, macronutrients such as nitrogen and silica, and micronutrients, especially iron (see reviews by *Francis et al.* [1998] and *Miller et al.* [2004]). Vertical mixing, and the mixed layer depth (MLD) in particular, is critical in linking the physical/chemical and biological processes [e.g., *Mann*, 1993; *Steele and Henderson*, 1993; *Gargett*, 1997]. If the mixed layer is too deep, phytoplankton will be transported beneath the euphotic zone inhibiting their growth due to the absence of light. Shallow mixed layers may lie above the nutricline or overlay a statically stable layer, and thus phytoplankton will consume the nutrients faster than they can be entrained into the surface layer from below, thereby limiting photosynthesis. In addition, if the MLD is sufficiently shallow in late winter for photosynthesis to occur and the resulting phytoplankton biomass is adequate to sustain zooplankton populations, then when the mixed layer shoals in spring, grazing by zooplankton can limit algal biomass [e.g., *Evans and Parslow*, 1985; *Frost*, 1991; *Fasham*, 1995].

[6] Several studies have emphasized the impact of changes in MLD during 1976–1977 on the lower trophic levels of the North Pacific ecosystems [*Venrick et al.*, 1987; *Polovina et al.*, 1994]. *Brodeur and Ware* [1992] hypothesized that changes in wintertime MLD over the northeast Pacific could impact the micronutrient supply and/or change the rate of primary productivity and the efficiency of zooplankton grazing in spring. *Polovina et al.* [1995] indicated that shoaling of the mixed layer in winter post 1976–1977 could significantly enhance productivity in the Gulf of Alaska by increasing the light available for photosynthesis based on MLDs estimated from temperature profiles and a plankton population dynamics model. However, the MLD is influenced by salinity in subarctic waters, and it is unclear whether there is sufficient variability in the late winter MLD in the northeast Pacific to significantly impact primary and secondary production [*McClain et al.*, 1996].

[7] The mixed layer depth is regulated by wind stirring, buoyancy forcing via surface heat and freshwater fluxes, and the density jump at the base of the mixed layer [*Alexander et al.*, 2000]. The latter influences MLD since turbulence may not be able to penetrate into a statically stable layer. During late winter in the subarctic North Pacific the mixed layer extends down to the upper portion of the halocline, located between depths of approximately 70 and 120 m [*Roden*, 1964; *Freeland et al.*, 1997; *de Boyer Montégut et al.*, 2004]. Thus low-frequency changes in the Ekman pumping in the Gulf of Alaska, which vertically displaces the halocline, may impact the wintertime MLD by moving a layer with strong density gradients toward or away from the surface. After the mid-1970s the pycnocline was shallower in the central part of the Gulf of Alaska and deeper in a broad band along the coast, primarily due to the local response to Ekman pumping [*Cummins and Lagerloef*, 2002; *Capotondi et al.*, 2005]. The extent to which this halocline variability impacts the MLD in the northeast Pacific is an open question.

[8] Decadal changes in the physical state of the North Pacific Ocean during the 1976 transition and their impact on the phytoplankton and zooplankton were simulated by *Haigh et al.* [2001] and *Chai et al.* [2003] using an ecosystem model embedded in an ocean general circulation model (OGCM). *Haigh et al.* [2001] performed simulations for 1952–1975 and for 1977–1989 using the mean atmospheric forcing over those two periods. The model reproduced the observed increase in phytoplankton in the central Pacific in summer and a southward displacement of the subtropical chlorophyll front in all seasons in the later period relative to the earlier one. The model also indicated an increase in zooplankton over the eastern subarctic Pacific in summer after 1976, but the magnitude and pattern of the increase differed from the observed values by *Brodeur and Ware* [1992]. *Chai et al.* [2003] used time-dependent forcing and substantially different physical and biological components than *Haigh et al.* [2001] to investigate variability in the subtropical chlorophyll front. They found that the front expanded and extended farther south after the 1976–1977 shift, in agreement with *Haigh et al.* [2001]. In the present study, we use the model simulation described by *Chai et al.* [2003] to investigate the physical and biological changes in the northeast Pacific Ocean, especially those which occurred across the 1976–1977 transition.

2. Model Simulation

[9] The physical component of the model, which simulates temperature, salinity, and currents, is the National Center for Atmospheric Research (NCAR) Climate System Model Ocean Model (NCOM) described by *Large et al.* [1997] and *Gent et al.* [1998]. NCOM is derived from the Geophysical Fluid Dynamics Laboratory (GFDL) Modular Ocean Model with the addition of a mesoscale eddy flux parame-

terization along isopycnal surfaces [*Gent and McWilliams*, 1990] and a nonlocal planetary boundary layer parameterization [*Large et al.*, 1994]. The advection of tracers, including temperature, salinity, and the biogeochemical components, is calculated using a third-order upwind differencing scheme. The background horizontal and vertical mixing coefficients for all tracers are 2.0×10^6 cm^{-2} s^{-1} and 0.1 cm^{-2} s^{-1}, respectively. The version of the model used here, described by *Li et al.* [2001], covers the Pacific from 45°S to 65°N and from 100°E to 70°W with realistic geometry and bathymetry. There is no flow through the boundaries, and a sponge layer, where the model's temperature, salinity, nitrate, and silicate are relaxed toward observations, is applied within 10° of the meridional boundaries. The longitudinal resolution is a uniform 2°. The latitudinal resolution is 0.5° within 10° of the equator, gradually increases to 2° within 20° of the equator, and is fixed at 2° north of 20°N and south of 20°S. There are 40 vertical levels, with 23 levels in the upper 400 m. The model's relatively coarse horizontal and vertical resolution allows us to examine basin-scale variability over an extended period of time but is not sufficient to resolve eddies or coastal processes.

[10] The biological model, developed by *Chai et al.* [2002], consists of 10 compartments, with "small" and "large" classes of phytoplankton (P1, P2) and zooplankton (Z1, Z2), two forms of dissolved inorganic nitrogen (nitrate (NO_3) and ammonium (NH_4)), detrital nitrogen (DN), silicate ($Si(OH)_4$), detrital silicon (DSi), and total carbon dioxide (TCO_2). Small phytoplankton (P1) have variable growth rates that depend on temperature, nitrogen, and light. Their biomass is regulated by micrograzers (Z1), while their net productivity is largely remineralized [*Landry et al.*, 1997]. The large phytoplankton class (P2 > 10 μm) represents the diatom functional group, which can grow rapidly under optimal nutrient conditions [*Coale et al.*, 1996]. Iron and its limitation on phytoplankton growth are not modeled directly but are treated implicitly via two parameters: the slope of the photosynthetic rate over irradiance at low irradiance and the maximum phytoplankton growth rate [*Chai et al.*, 2002, 2007]. The parameter values, which are constant in space and time, were derived from the limited number of lab and field experiments and from model experiments in which iron was added to the equatorial Pacific [*Chai et al.*, 2007]. The micrograzers have growth rates similar to P1 and grazing rates (G1) that depend on the density of both P1 and Z1 [*Landry et al.*, 1997]. The mesozooplankton (Z2) graze on P2 and DN and prey on Z1 and have a feeding threshold based on conventional grazing dynamics [*Frost and Frazen*, 1992]. The loss of Z2 from the system, primarily due to predation from higher trophic levels, is represented by a quadratic expression. Sinking particulate organic matter is converted to inorganic nutrients via regeneration, similar to the process described by *Chai et al.* [1996]. Nitrogen is the "currency" in the ecosystem model; that is, plankton biomass and detritus pools are in units of millimoles of nitrogen per cubic meter (mmol N m^{-3}). A detailed discussion of the model equations and parameter values is given by *Chai et al.* [2002].

[11] The model's temperature, salinity, and nutrients were initialized using climatological values from the National Ocean Data Center (NODC), while the biological components were assigned a value of 0.025 mmol m^{-3} at the surface, decreasing exponentially with a scale length of 120 m: the average depth of the euphotic zone. The full model was then integrated for 10 years with climatological forcing, during which it reached a stable annual cycle in the upper ocean [*Chai et al.*, 2003]. During this spin-up period and in the subsequent model experiment the physical and ecosystem components were integrated synchronously.

[12] In the simulation examined here, the model is forced with observed atmospheric fields over the period 1955–1999, and the output is archived monthly during 1960–1999, allowing for a 5-year spin-up period. The surface fluxes of momentum, heat, fresh water, and insolation used to drive the model were derived from monthly mean values obtained from the Comprehensive Ocean Atmosphere Data Set (COADS) [*da Silva et al.*, 1994] during 1955–1993 and from the National Center for Environmental Prediction (NCEP) reanalysis [*Kalnay et al.*, 1996; *Kistler et al.*, 2001] during 1993–1999. The monthly means were subsequently interpolated to daily values. The heat flux includes shortwave and longwave radiation and the sensible and latent heat flux. The sensible (latent) fluxes are computed using the observed air temperature (specific humidity) and the model's SST. The model does not include the diurnal cycle, so the daily averaged insolation is multiplied by 0.5 to determine the photosynthetically available radiation (PAR, wavelengths between 400 and 700 nm). PAR decreases exponentially with depth because of absorption and scattering by water and phytoplankton.

[13] The model is forced by the observed difference between precipitation and evaporation. Since precipitation is not well measured over the ocean, the salinity of the surface layer is also relaxed to the observed climatological monthly mean values [*Levitus et al.*, 1994] using a 30-d timescale. While this damping greatly reduces the surface salinity variability, the deeper ocean, including the halocline, is relatively unconstrained. *Li et al.* [2001] and *Chai et al.* [2003] provide more detailed descriptions of the procedures used to initialize and force the model and its fidelity in simulating the physical and biological state of the Pacific Ocean.

3. Results

3.1. SST Changes

[14] We will mainly focus on the years 1970–1976 and 1977–1988 since they were dominated by opposite phases of the PDO [*Bond et al.*, 2003] and because the fields used to force the model during these years were all derived from COADS (NCEP reanalysis is used to drive the model after 1993). The epoch difference (Δ, defined as 1977–1988 minus 1970–1976 from here on) in the observed and simulated North Pacific SST (°C) during February, March, and April (FMA) is shown in Figure 1. In both observations and the OGCM, negative ΔSST values in the central and western Pacific between approximately 25°N and 45°N are ringed by positive ΔSST values over the remainder of the North Pacific, indicative of a change to the positive phase of the PDO after 1976. The model also reproduces several of the finer-scale features of the ΔSST field, with negative centers at 30°N, 155°W and 40°N, 175°E and positive centers in the vicinity of the Alaskan Peninsula and Baja California. The latter is part of a broad swath the extends

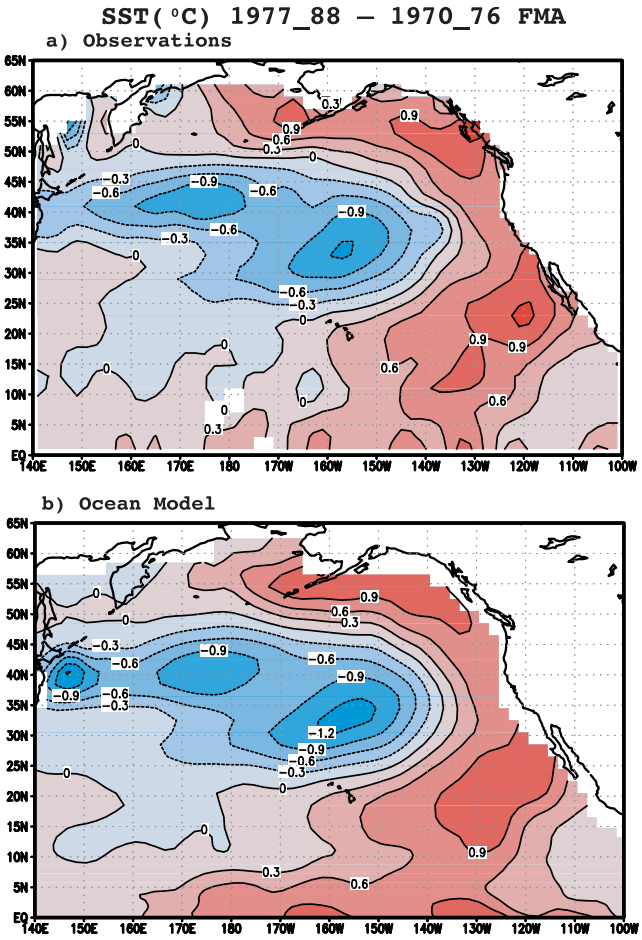

Figure 1. Epoch difference, 1977–1988 minus 1970–1976 (Δ), in SST (°C) during February, March, and April (FMA) from (a) observations and (b) the model simulation. The observed values are from COADS.

over much of the tropical Pacific suggesting that the PDO is part of a larger pattern that includes the tropics as well as the North Pacific, consistent with the findings of *Zhang et al.* [1997], *Newman et al.* [2003], and *Deser et al.* [2004]. The close correspondence between the observed and simulated ΔSST fields provides some confidence in the GCM's ability to simulate decadal changes in the northeast Pacific, although using the observed air temperature to compute the surface fluxes partially constrains the SSTs to track observations [e.g., *Seager et al.*, 1995].

3.2. Physical-Biological Linkages

[15] A number of studies, including those by *Brodeur and Ware* [1992], *Polovina et al.* [1995], and *Freeland et al.* [1997], indicated that surface mixing in winter has a strong impact on the Gulf of Alaska ecosystem over the course of the seasonal cycle. The ΔMLD (m) during FMA is shown for the GOA (contours) in Figure 2, where the MLD is defined as the depth where the potential density is 0.125 kg m^{-3} greater than the surface value. The mixed layer shoals by more than 20 m in the central gulf in 1977–1988 relative to 1970–1976, a reduction of ~30%, and decreases by ~12 m at 50°N, 145°W (location of ocean station P), consistent with the observational analysis of *Li et al.* [2005]. Unlike the central North Pacific, where there is a robust inverse relationship between SST and MLD anomalies [e.g., see *Deser et al.*, 1996], the shoaling in the central GOA occurs near the nodal line for decadal SST changes (compare Figure 1 and Figure 2), and ΔSST and ΔMLD are both positive along the North American coast.

[16] The MLDs in February and in FMA are overlain on the temperature and salinity profiles in FMA from 1960 to 1999 averaged over a region (46–52°N, 160–140°W, box in Figure 2) in the central GOA (Figure 3). The MLD, which extends to the upper portion of the halocline, closely tracks the vertical variations in salinity but not temperature, including the epoch changes in the halocline around 1976. The close correspondence between MLD and the halocline occurs even though the salinity variations near the surface are negligible in the model because of the strong restoring of the surface salinity toward climatology. Furthermore, the epoch difference in salinity, at depths of 70 to 150 m, closely resemble the MLD pattern, with increased salinity in the center of the gyre and decreased salinity along the coast (not shown). The shoaling of the halocline and hence the mixed layer depth result from upward vertical velocity (w) in the central/western GOA in 1977–1988 relative to 1970–1976 (Figure 4). The upward vertical motion is driven by enhanced Ekman pumping associated with a deeper Aleutian Low after 1976 [*Lagerloef*, 1995; *Cummins and Lagerloef*, 2002; *Chai et al.*, 2003; *Capotondi et al.*, 2005].

[17] Changes in MLD can influence primary productivity by regulating the amount of light and nutrients available for photosynthesis. In the northeast Pacific the highest primary productivity (PP) integrated over the upper 100 m of the model occurs in March–May (monthly production and grazing rates are presented in section 3.3). The epoch difference in primary productivity (ΔPP in mmol N m^{-2} d^{-1}) during March, April, and May is also shown in Figure 2. The ΔPP pattern, with a decrease in the central GOA ringed by an increase along the

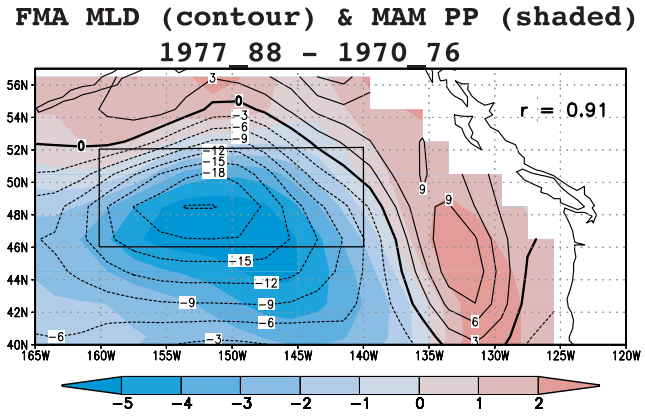

Figure 2. ΔMLD (m; contours) in FMA and ΔPP (C m^{-2} d^{-1}; shaded) in March, April, and May integrated over the upper 100 m of the ocean. The PP values have been spatially smoothed using a nine-point filter and converted from nitrogen to carbon by multiplying them by 6.625 as indicated by the Redfield ratio. The box indicates the central Gulf of Alaska (GOA) region.

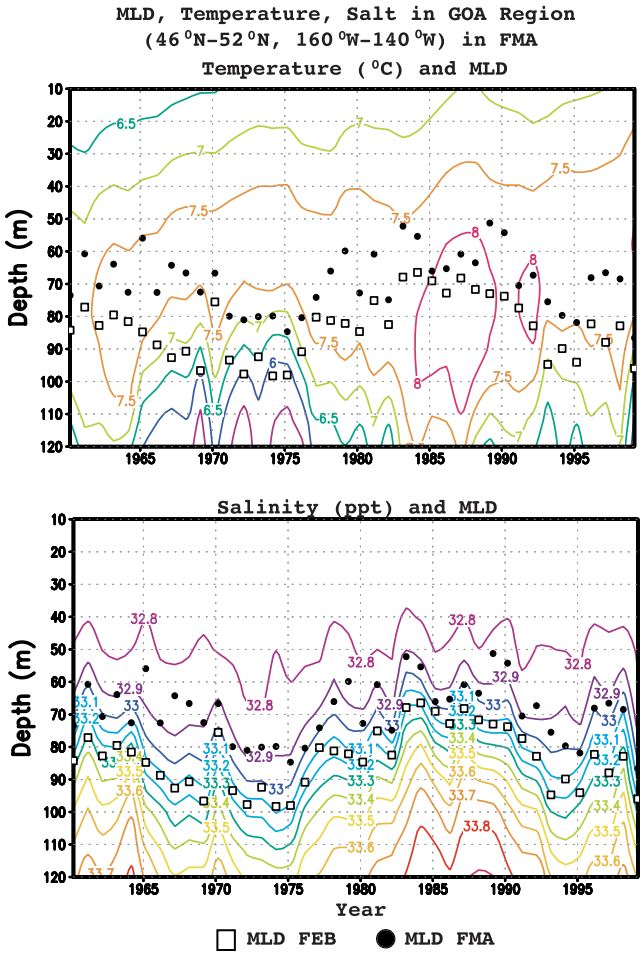

Figure 3. (a) Temperature (°C) and (b) salinity (ppt) over the upper 120 m of the ocean during FMA in the central GOA region (46–52°N, 160–140°W) for 1960–1999. The MLDs during February and FMA are shown by open squares and solid circles, respectively.

coast, is remarkably similar to the structure of ΔMLD; indeed, the pattern correlation between the two is 0.91.

[18] The positive correlation between MLD and PP initially suggested to us that vertical mixing of nutrients into the surface layer (i.e. deeper MLD causes increased entrainment of nutrients which causes greater PP and vice versa) might have caused the simulated biological changes in 1977–1988 relative to 1970–1976 in the GOA. Nitrate is an essential nutrient for both phytoplankton groups, while silica is an important structural element for diatoms, represented by the large phytoplankton group. The nitrate (NO_3) and dissolved silica (H_4SiO_4) concentrations (mmol m^{-3}) during FMA are shown for the average over the 1977–1988 period (contours) and for 1977–1988 minus 1970–1976 (shading) in Figure 5. There is a small reduction in both nitrate and silica in the central GOA after 1976, where the decrease in NO_3 at 50°N, 145°W is consistent with station P data [cf. *Freeland et al.*, 1997]. However, the ΔNO_3 and ΔH_4SiO_4 are small fractions (<10%) of the mean concentration of nutrients during 1977–1988. The pattern of the epoch shift in the nutrient concentrations is also quite different from the change in primary productivity. For example, the greatest

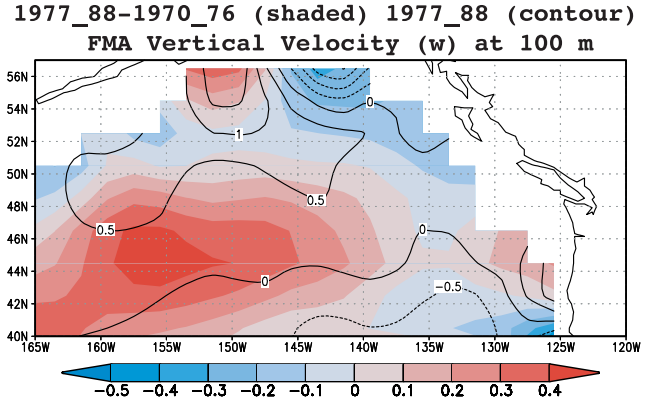

Figure 4. The 1977–1988 mean (contours) and Δ (shading) vertical velocity ($w \times 10^{-6}$ m s^{-1}) at 100 m depth during FMA. Positive values indicate upward motion.

decrease in primary productivity occurs in the vicinity of 46°N, 150°W (Figure 2), where both NO_3 and H_4SiO_4 strongly increase, as does the flux across the nutricline (given by $w\ \partial(NO_3)/\partial z$ at 100 m, not shown), which resembles the vertical motion field in Figure 4. Finally, the concentrations of both NO_3 and H_4SiO_4 exceed 5 mmol m^{-3} over most of the northeast Pacific during 1977–1988, sufficient to maintain rapid phytoplankton growth [*Chai et al.*, 2002]. Thus the change in nutrients does not appear to be responsible for the general reduction in productivity after 1976 in the central GOA.

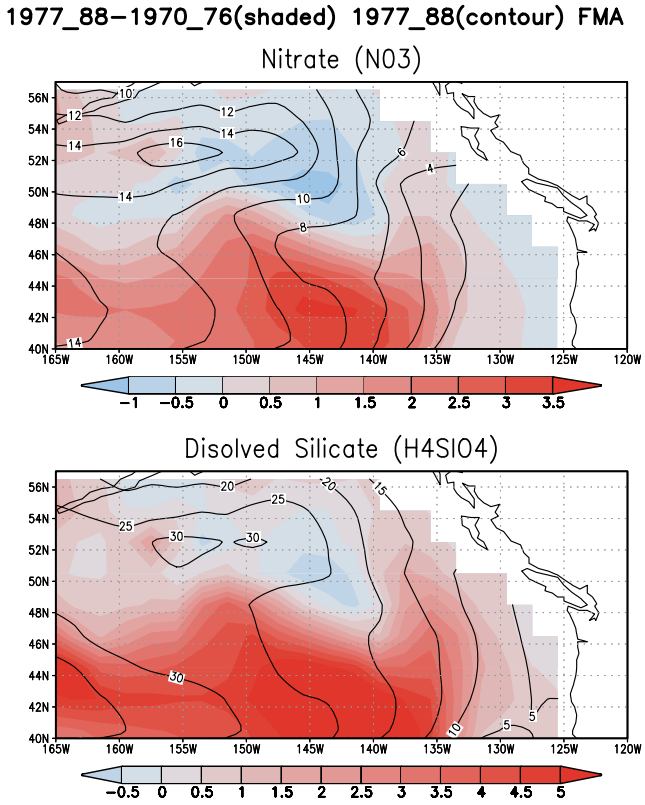

Figure 5. The 1977–1988 mean (contours) and Δ (shading) for (a) nitrate (NO_3) and (b) dissolved silica (H_4SiO_4) concentrations (mmol m^{-3}) during FMA.

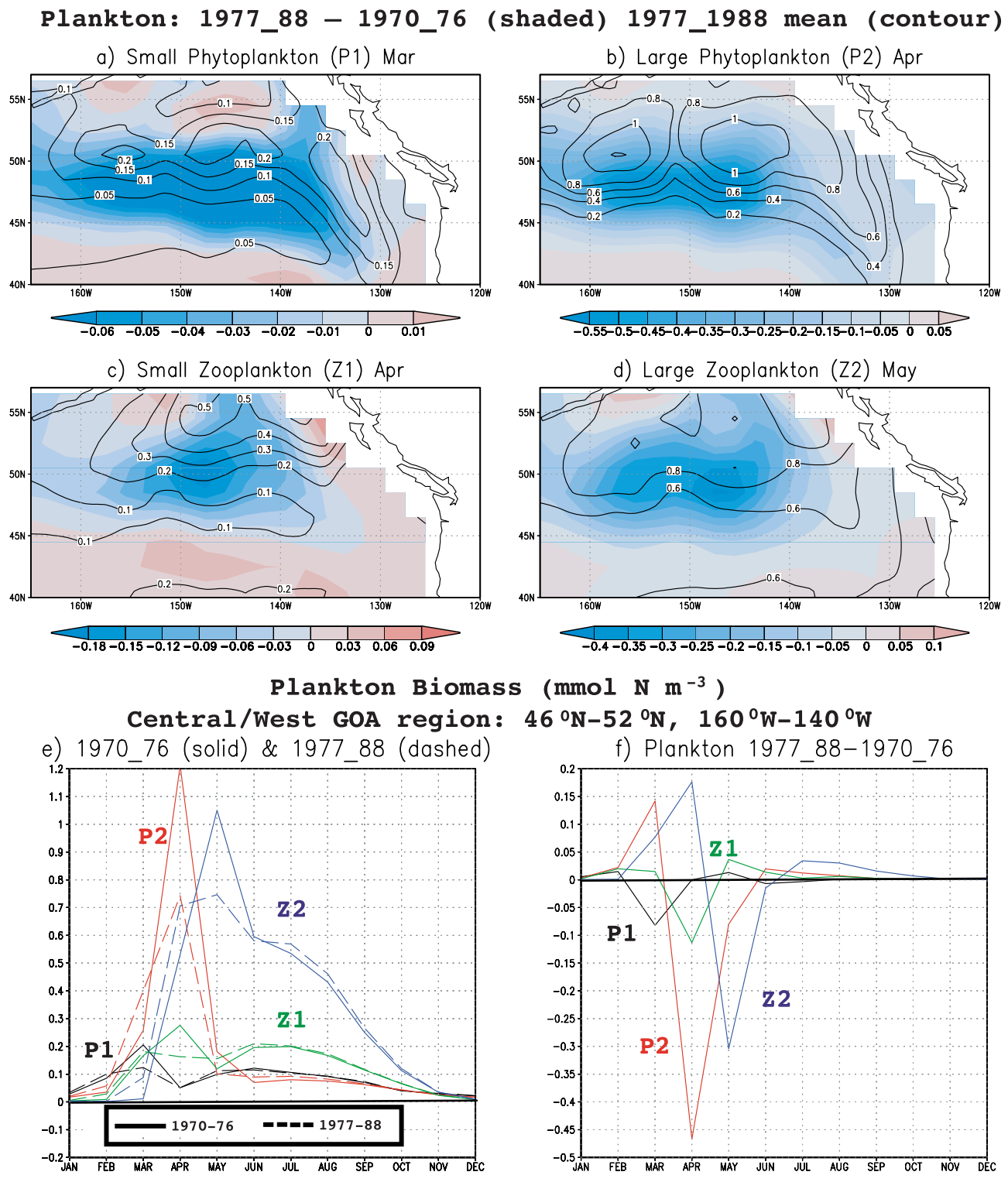

Figure 6. The 1977–1988 mean (contours) and Δ (shading) for (a) small phytoplankton (P1) in March, (b) large phytoplankton (diatoms, P2) in April, (c) small zooplankton (Z1) in April, and (d) large zooplankton (Z2) in May. Also shown are the values of P1, P2, Z1, and Z2 for each calendar month for the periods (e) 1970–1976 and 1977–1988 and (f) Δ, the difference between the two periods. The P and Z values (mmol N m^{-3}) presented here and Figures 7–9 are from the top model level.

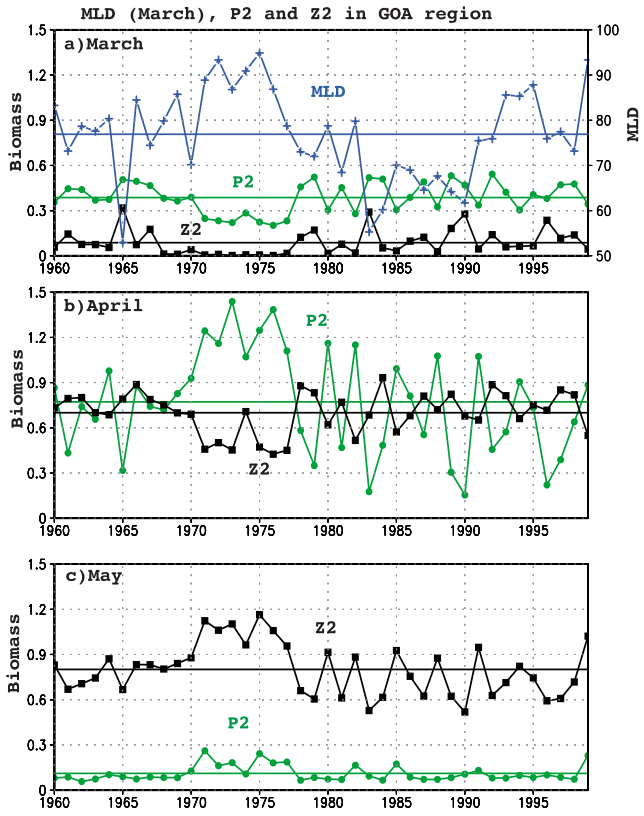

Figure 7. P2 and Z2 biomass (mmol N m^{-3}) from 1960–1999 averaged over the central Gulf of Alaska region for the months of (a) March, (b) April, and (c) May, along with the MLD (m, scale on right axis) in (Figure 7a) March. Also shown are the MLD, P2, and Z2 means (thin lines) over the 1960–1999 period.

3.3. MLD, Light Regulation, and Trophic Interactions

[19] What is the primary factor linking the epoch difference in MLD with primary productivity in the GOA if it is not a change in (macro) nutrients? One possibility is that changes in MLD impact phytoplankton by altering the light available for photosynthesis, followed by trophic interactions that modify the initial biological response as the seasonal cycle progresses. Specifically, a shoaling of the wintertime MLD in 1977–1988 relative to 1970–1976 leads to more light and thus enhanced primary productivity and greater phytoplankton biomass earlier in the year in the central GOA region. The resulting increase in phytoplankton enhances the food supply enabling a more rapid rise in the zooplankton biomass, but the associated increase in grazing subsequently suppresses phytoplankton and then zooplankton biomass during their peak in spring.

[20] To test this hypothesis, we first examine if the epoch changes are coherent across trophic levels and if these changes vary over the seasonal cycle. The 1977–1988 mean and Δ in biomass are shown in Figures 6a–6d for each of the four plankton classes over the northeast Pacific. (The mean values during 1977–1988 are similar to those from the entire 1960–1999 record, not shown.) The biomass values (mmol N m^{-3}) of the four plankton classes are presented for the calendar month in which they reach a maximum: March for small phytoplankton (P1), April for small zooplankton (Z1) and large phytoplankton (P2), and May for large zooplankton (Z2). The biomass shown in Figure 6 (and from here on) is obtained from the surface layer (0–10 m) of the model, where the epoch differences are largest. The mean P1 and P2 biomasses (contours) peak at ~50°N, while the Z1 and Z2 reach maximum values north of ~52°N.

[21] The mean plankton biomass during the two periods and the difference between them are presented as a function of calendar month for the central GOA region in Figures 6e and 6f, respectively. The pronounced mean seasonal cycle of zooplankton, with a maximum in May, is consistent with observations at station P [cf. *Brodeur et al.*, 1996; *Mackas et al.*, 1998]. The mean plankton biomass, however, is greater than that observed during the warm season; that is, P is approximately twice that measured at station P during April–June [*Chai et al.*, 2003]. Additionally, spring blooms are not commonly observed in the central GOA [*Boyd and Harrison*, 1999; *Brickley and Thomas*, 2004]. The overabundance of plankton, and P2 in particular, is likely due to the treatment of iron-limited growth in the model, as discussed further in section 4.

[22] The Δ biomass for all four plankton classes (shading in Figure 6) is negative and of large amplitude relative to the mean, indicating a substantial decrease in biomass after 1976. For example, P2 decreases by more than 60% in the vicinity of 46°N, 150°W during April. The reductions in phytoplankton and zooplankton biomass are collocated, and both are centered within and slightly to the south of the maximum in the long-term mean. The P and Z biomass in the central GOA region decreases by ~40% in 1977–1988 relative to 1970–1976 during its spring peak (Figures 6e and 6f). This decrease is both preceded and followed by an increase in biomass in all four plankton classes, although the increase is relatively small except for P2 and Z2 in March and April, respectively. The spatial coherence of ΔP and ΔZ and the reversal in sign of the Δ in biomass with month are consistent with our hypothesis that trophic interactions and their evolution over the seasonal cycle play an important role in modulating the low-frequency ecosystem variability.

[23] Given that the magnitude of the mean and the epoch difference in biomass are much greater for the larger plankton classes (Figure 6), we focus on the dynamics of P2 and Z2 from here on. The time series of the P2 and Z2 biomass (mmol N m^{-3}) from 1960 to 1999 averaged over the central Gulf of Alaska region for the months of March, April, and May, along with the MLD (m) in March, are shown in Figure 7. The MLD is deeper than normal during the early epoch, except for 1970, and shallower than normal during later epoch, except for 1977, 1980, and 1982, which are near normal. There is an inverse relationship between MLD and P2 biomass (Figure 8a) as reflected by a −0.67 correlation between the two over the entire record (significant at the 99% level allowing for autocorrelation in the time series [e.g., see *Wilks*, 1995]). The phytoplankton biomass in March is below normal for all years between 1971 and 1976, but it is near normal and has much greater interannual variability during 1977–1988, which suggests that the deeper mixed layer during the first period has a greater impact on photosynthesis and phytoplankton bio-

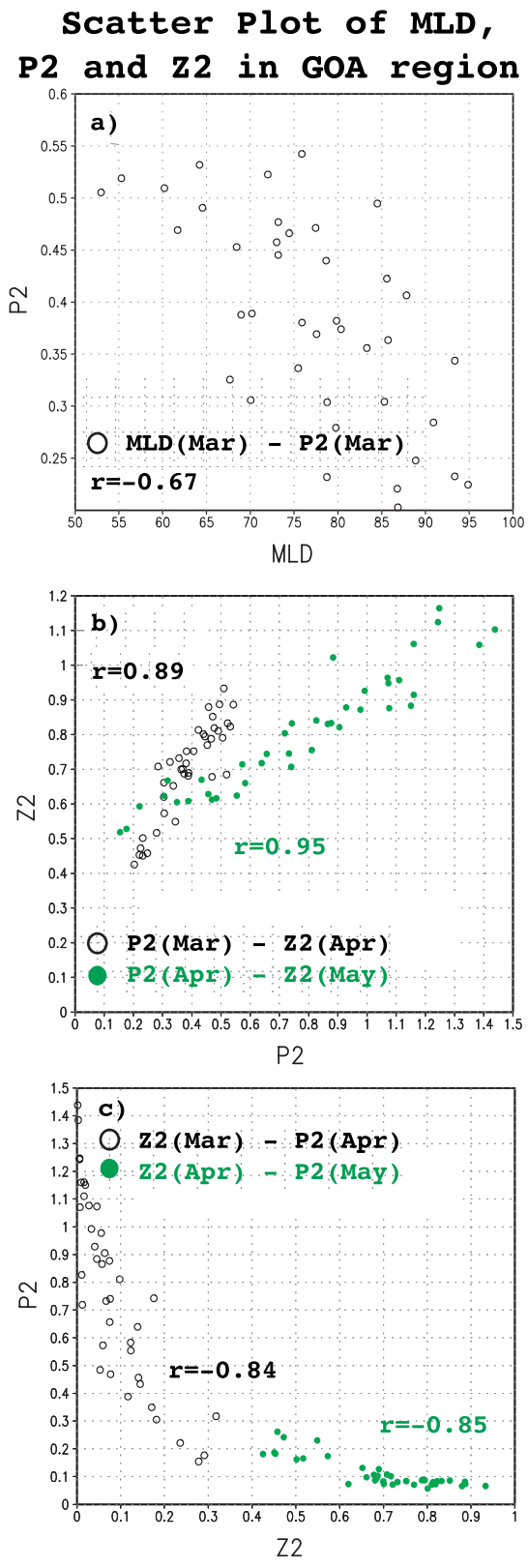

Figure 8. Scatterplots of (a) MLD (March) with P2 (March), (b) P2 (March) with Z2 (April) and P2 (April) with Z2 (May), (c) Z2 (March) with P2 (April) and Z2 (April) with P2 (May). MLD (m) and P2 and Z2 (mmol N m^{-3}) values are for the central GOA region for the years 1960–1999. Correlation (r) values between the variables are also given.

mass than the shallower mixed layer in the later period. The asymmetry in the relationship between MLD and P2 biomass is also indicated by a scatterplot of the two variables averaged over the GOA region during March, where P is nearly independent of MLD for depths <∼65 m (Figure 8a). The existence of a threshold depth, however, is difficult to determine given the scatter in Figure 8a, i.e., the P2 variability that is unrelated to MLD and the small number of relatively shallow MLD values.

[24] In winter the phytoplankton and zooplankton biomasses are low and vary together in the GOA region (Figures 7a, 9b, and 9c); for example, the correlation between P2 and Z2 in March is 0.72. The positive correlation suggests that grazing is not controlling phytoplankton biomass accumulation. While the Z2 biomass is generally low during March, it is nearly zero during 1970–1976 (Figures 6e and 7a). Very low zooplankton abundance in winter can be a critical factor in enabling rapid phytoplankton growth in spring (Figure 8c) [*Evans and Parslow*, 1985; *Frost*, 1991; *Fasham*, 1995]. Indeed, the P2 biomass switches from well below normal in March to well above normal in April during 1970–1976 (Figure 7b). The Z2 biomass remains anomalously low in April, reflecting the limited food supply in the previous month. Following the increase in P2 biomass in April, the Z2 biomass in May is above normal during the early 1970s. In contrast to 1970–1976, neither P2 nor Z2 exhibit significant changes in the mean during 1977–1988; rather, they exhibit large interannual variability.

[25] The lagged P-Z relationships during 1970–1976 in March through May are also very robust over the entire 40-year record, as indicated by the limited scatter between P2 and Z2 (Figures 8b and 8c). The P2(March)-Z2(April) and P2(April)-Z2(May) correlations are 0.89 and 0.95, respectively, while the Z2(March)-P2(April) and Z2(April)-P2(May) correlations are both ∼−0.85. The relationship between P2 with Z2 in the following month appears to be linear (Figure 8b), with a greater change in Z2(April) relative to a unit change in P2(March) than for Z2(May) relative to P2(April). While a linear relationship provides a reasonable fit for Z2(March)-P2(April) and for Z2(April)-P2(May), the two combined suggest a decreasing exponential function (Figure 8c). The concurrent P2-Z2 correlations in the GOA region are −0.72 and 0.77 in April and May, respectively. While significant, the change of sign between months and the slight decrease in magnitude compared to the lag correlations suggest that the concurrent P-Z correlation values during spring reflect the lag relationship between the two trophic levels. However, we may not be fully resolving the period of the lag with monthly data.

[26] The magnitude of the lead-lag correlations between P and Z at individual grid points generally exceeds 0.4 over the most of the northeast Pacific and 0.6 in the central and western GOA (not shown). Consistent with the regional analyses, the 1-month lag P2-Z2 correlations are positive, and the Z2-P2 correlations are negative for both March to April and April to May.

[27] The timing of the mixed layer depth and the plankton changes with respect to the seasonal cycle are examined further in Figure 9 using time-latitude (Hovmöller) diagrams of monthly mean (contours), Δ (shaded) values of

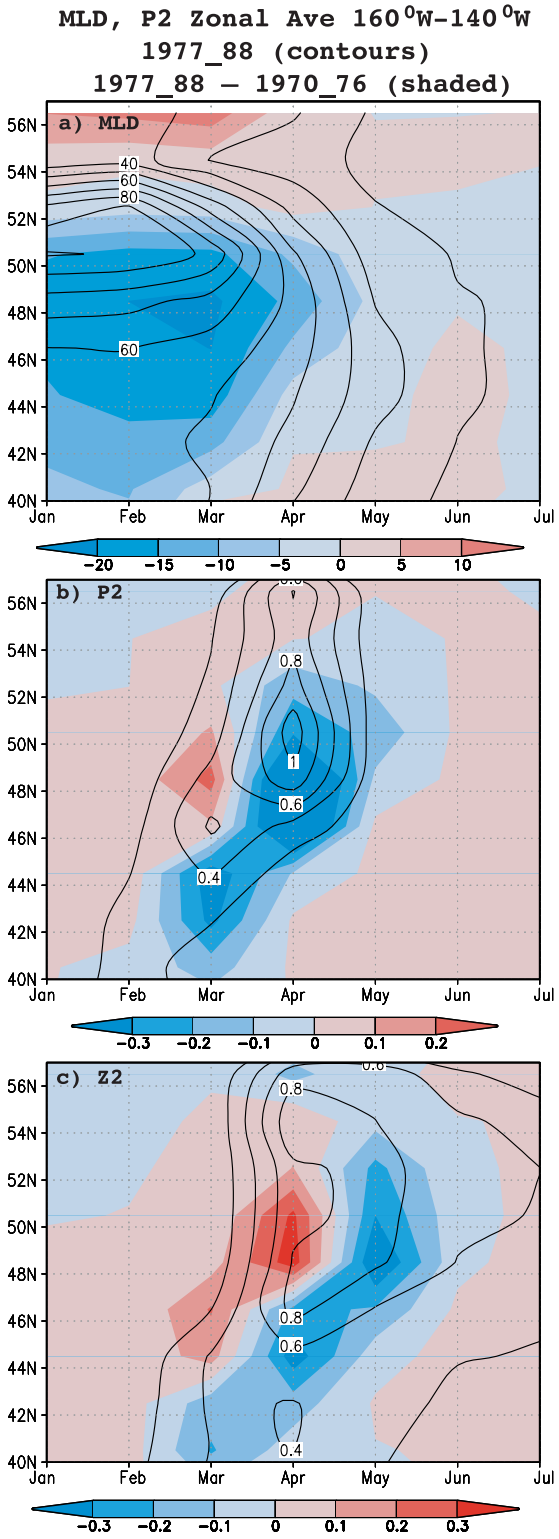

Figure 9. Hovmöller (latitude-time) diagrams of the 1977–1988 mean (contours) and Δ (shaded) values of (a) MLD (m), (b) P2 (mmol N m^{-3}), and (c) Z2 (mmol N m^{-3}). The values are averaged over 160–140°W and shown for January through July.

MLD, and P2 and Z2 biomass. The variables are averaged over 160–140°W and presented for 40–57°N from January through July. The maximum mean MLD exceeds 80 m during January–March in the vicinity of 50°N and then decreases at all latitudes to about 10–20 m by May. The mean P2 biomass begins increasing in midwinter, reaching a maximum in February, March, and April for the latitude bands of 40–44°N, 44–47°N, and 48–57°N, respectively. In addition to the seasonal cycle in insolation, the canonical evolution of P2 also depends on MLD, which is shallower in the southern part of the domain in January, February, and March and thus more conducive for photosynthesis in a light-limited regime. The mean Z2 biomass increases during late winter, peaks from April to May, and then declines but much more slowly than P2.

[28] During January–March the ΔP2 biomass increases where the ΔMLD has decreased and vice versa, with the greatest increase in P2, located at 48°N in March, occurring in conjunction with the greatest decrease in MLD (shading, Figure 9). This inverse relationship between ΔMLD and ΔP2 occurs over most of the domain during winter and is consistent with changes in light limitation influencing phytoplankton growth on decadal timescales. However, this relationship breaks down in spring and south of ~46°N in late winter as light is less of a factor in regulating primary productivity and grazing by zooplankton may have already begun to constrain the phytoplankton biomass. As in the central GOA region, ΔP2 and ΔZ2 are enhanced prior to the annual mean peak in winter, reduced during and slightly after the peak in spring, and then weakly enhanced by July between 40°N and 56°N. For example, at 48°N the sharp increase in P2 in March is followed by a rapid rise in Z2 in April, while the decrease in P2 in April is followed by a decrease of Z2 in May.

[29] Primary productivity (PP) of P2 and grazing (G) of P2 by Z2 (mmol N m^{-2} d^{-1}) are shown for northeast Pacific during the months of February through May in Figure 10. The maximum PP averaged over the 1977–1988 period (contours) migrates from the southern to the northern edge of the GOA from February to May as the amount of light necessary for photosynthesis moves northward. This migration is not zonally uniform, as the largest values occur at different longitudes from February to May. The overall maximum mean PP occurs in April rather than June (not shown), suggesting that factors other than the availability of light are limiting phytoplankton growth in late spring and summer. In general, the mean PP and G patterns are very similar, although the latter is shifted south of the former but only by ~2° latitude. The collocation of PP and G is consistent with local grazing on P2 by Z2, since the plankton life cycles occur much faster than the advection by ocean currents. The slight southward displacement of G relative to PP is likely due to the initiation of photosynthesis earlier in the seasonal cycle and thus farther north relative to grazing by zooplankton, and so the spatial patterns of G in March and April resemble the PP pattern in the previous month.

[30] Like the mean values, ΔPP and ΔG (shading in Figure 10) also move northward across the GOA from February to May, and the grazing is shifted slightly south relative to the primary productivity. ΔPP and ΔG are generally positive to the north and negative to the south

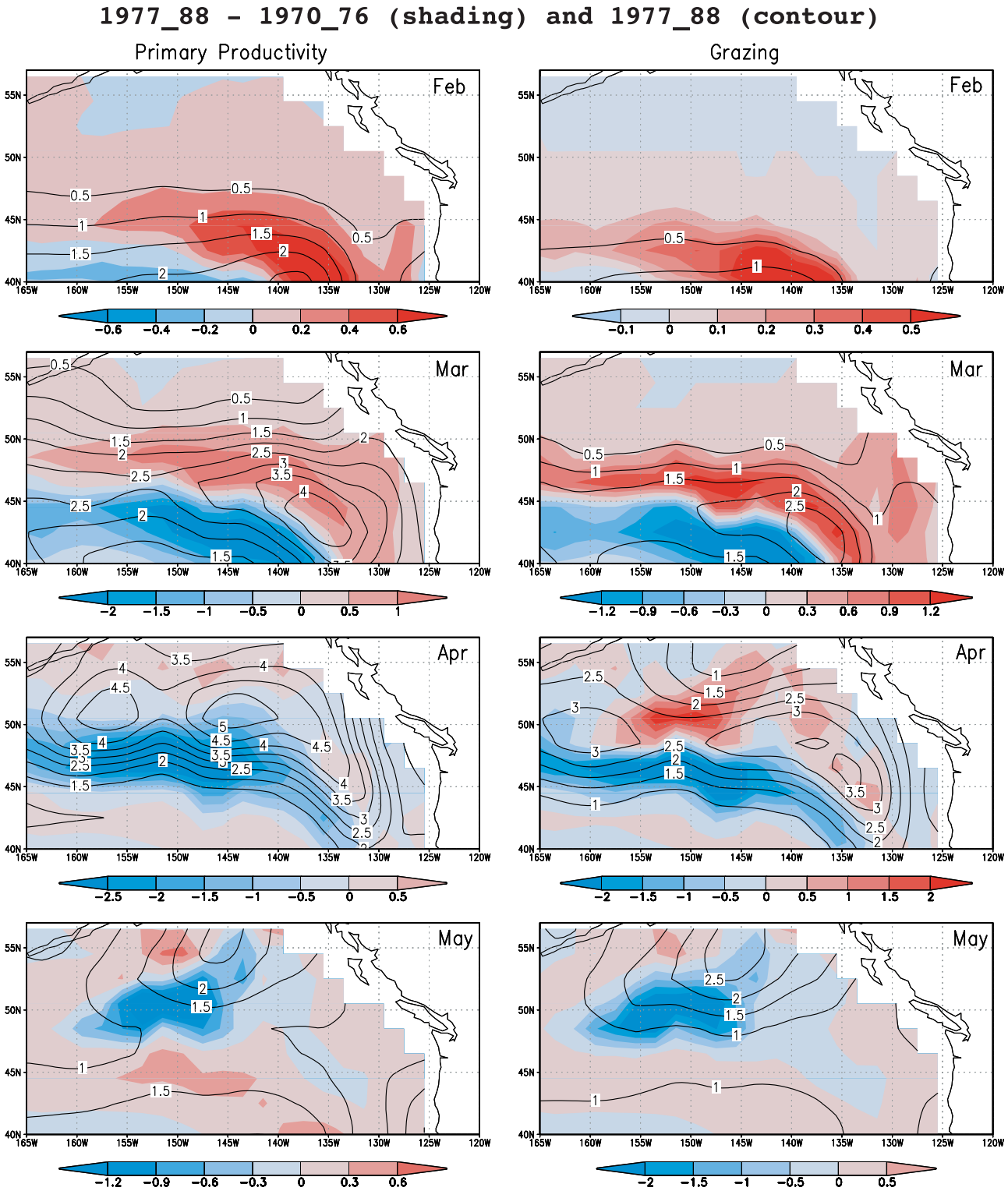

Figure 10. The 1977–1988 mean (contours) and Δ (shaded) (left) P2 primary productivity and (right) grazing of P2 by Z2 for the months of February, March, April, and May. The values have been integrated over the upper 100 m and are in units of mmol C m^{-2} d^{-1}.

of their respective maximum in the 1977–1988 mean values, indicating a northward displacement in biological activity after the 1976 regime shift. The epoch differences are also a substantial fraction of the mean; for example, primary productivity decreased by as much as ~70% in 1977–1988 relative to 1970–1976. There is generally a close correspondence between ΔPP and ΔG for each calendar month. Thus there is both enhanced PP and G

over much of the Alaskan Gyre during February through April after 1976. The increase in grazing is especially pronounced between 48°N–52°N and 145°W–155°W in March and April and likely contributes to the strong suppression of PP in May in the central GOA.

4. Summary and Conclusions

[31] We have used a physical-ecosystem model to examine whether changes in the physical environment associated with the 1976–1977 transition influenced the lower trophic levels of the food web and if so by what means. We hypothesize that the following chain of events led to the difference in the physical climate and biology in the central Gulf of Alaska in 1977–1988 relative to 1970–1976 in the model. The Aleutian Low strengthened [e.g., *Trenberth and Hurrell*, 1994] and the associated cyclonic winds accelerated the Alaskan Gyre and enhanced Ekman pumping [*Capotondi et al.*, 2005]. The resulting increase in upwelling caused the halocline to shoal in the center of the Alaskan Gyre. Thus the mixed layer, which extends to the upper portion of the halocline in winter, did not penetrate as deep. As a result, more phytoplankton remained in the euphotic zone, and primary productivity and phytoplankton biomass increased earlier in spring. The enhanced food supply led to an increase in zooplankton biomass, but then grazing pressure led to a strong (∼40%) decrease in phytoplankton by April followed by a reduction in zooplankton by May. The 1-month lag between P and Z in spring likely reflects the timescales set by photosynthesis and grazing, although this was based on monthly averaged data and does not consider all of the potential biological interactions in the system such as nutrient recycling. Finally, both ΔP and ΔZ reversed sign again by summer, with greater biomass in 1977–1988 relative to 1970–1976, in agreement with observations [*Brodeur and Ware*, 1992]. However, the simulated increase was modest, with ∼10% more zooplankton biomass in June–July during the later epoch, which was substantially smaller than the doubling in zooplankton biomass estimated by *Brodeur and Ware* [1992].

[32] The results presented here are dependent on the simulation of variability in both the physical and biological models. As in previous studies, the winter mixed layer depth appears to be a critical variable for ecosystem dynamics in the North Pacific. Decadal variability of MLD in the northeast Pacific depends on dynamical ocean processes that influence the density jump at the base of the mixed layer (and top of the halocline). Interannual and decadal changes in MLD and phytoplankton biomass in the GOA are inversely related, indicative of a light-regulated ecosystem as suggested by *Boyd et al.* [1995] and *Polovina et al.* [1995] but only during winter. Subsequent changes in grazing rates appear to cause larger changes in biomass during their spring peak, leading to a positive correlation between winter MLD and spring primary productivity/plankton biomass. The importance of grazing in regulating the spring plankton biomass in the northeast Pacific has been noted before in the context of the mean seasonal cycle using one-dimensional models [*Evans and Parslow*, 1985; *Frost*, 1991; *Fasham*, 1995] and a three-dimensional physical/biogeochemical model [*Gregg*, 2002]. The epoch differences in biomass can also be viewed as changes in the seasonal cycle with the spring transition, or alternatively the northward seasonal advance of primary and secondary production, beginning earlier in the year in 1977–1988 relative to 1970–1976. *Mackas et al.* [1998], *Stabeno and Overland* [2001], and *Bograd et al.* [2002] have also found that decadal variability in the North Pacific climate and ecosystems can be manifest in the seasonal cycle, where the timing of lower trophic level production can be crucial to the higher trophic level organisms that prey upon them.

[33] On the basis of previous analyses [e.g., *Bond et al.*, 2003] and the simulation of SST in the OGCM we selected 1970–1976 and 1977–1988 as periods that exhibited "regime-like" behavior, i.e., when anomalies are of one sign. This appeared to be a fairly reasonable assumption for MLD depth, which is shallow (deep) during 1977–1988 (1970–1976) in the central GOA. However, the biological anomalies were consistent in sign only for 1970–1976; during 1977–1988, phytoplankton and zooplankton biomass were close to their long-term means and exhibited substantial interannual variability. The high degree of interannual variability during the later period has important implications for assessing regimes on the basis of observations: Insufficient sampling could lead to inaccurate estimates of the actual mean value over a given period. The reason for the difference in variability between epochs is unclear, although it may be due to a nonlinear relationship between MLD and primary productivity; that is, the phytoplankton is much more sensitive to changes in the March MLD when the latter exceeds ∼65 m in the GOA region. Perhaps when the MLD is above this threshold depth, enough light is available to sustain phytoplankton growth and thus is not as strong as a controlling factor. However, this hypothesis needs to be confirmed by future research.

[34] The model used in the present study may not adequately represent several potentially important processes, including eddies, near-shore processes such as coastally trapped waves, and zooplankton behavior and their interactions with higher trophic levels. The results may also be influenced by errors in the surface fluxes as well as deriving the surface fluxes from monthly data, thereby limiting strong episodic forcing. In addition, the eastern subarctic Pacific is a high-nutrient, low-chlorophyll (HNLC) region where micronutrients, especially iron, are believed to limit the growth of phytoplankton in late spring and summer [*Martin and Fitzwater*, 1988; *Boyd et al.*, 1996; *Harrison*, 2006]. The model's implicit treatment of iron limitation may be adequate for the equatorial Pacific [*Chai et al.*, 2002, 2007] but appears too weak in the northeast Pacific. This may have led to an overestimate of the simulated change in primary productivity and plankton biomass in response to the physical changes in the system. However, the processes identified here are still likely to play an important role in decadal variability in the GOA, since the lack of sunlight in conjunction with low iron levels may colimit growth in winter [*Maldonado et al.*, 1999] and grazing in combination with the limited iron supply may modulate spring blooms [*Frost*, 1991; *Fasham*, 1995; *Aumont et al.*, 2003]. While the direct simulation of the iron cycle has recently been included in OGCMs [*Aumont et al.*, 2003; *Gregg et al.*, 2003; *Moore et al.*, 2004], several key processes that influence iron cycling in the

marine environment are poorly known and thus crudely parameterized. Questions remain regarding the bioavailability, cellular quotas, and abiotic scavenging of iron and the magnitude of its external sources [*Johnson et al.*, 1997; *Fung et al.*, 2000; *Johnson et al.*, 2002]. Thus the role of iron limitation and small-scale/coastal processes upon decadal variability in the North Pacific Ocean warrants further exploration.

[35] **Acknowledgments.** We thank James Scott for his assistance in processing the data and drafting the figures and Yi Chao and collaborators for developing the OGCM and sharing the output with us. Comments from Hal Batchelder and two anonymous reviewers helped to improve the manuscript. This research received financial support from the NOAA office of Polar Programs, NASA's IDS program, and the NSF Oceans program.

References

Alexander, M. A., J. D. Scott, and C. Deser (2000), Processes that influence sea surface temperature and ocean mixed layer depth variability in a coupled model, *J. Geophys. Res.*, *105*, 16,823–16,842.

Aumont, O., E. Maier-Reimer, S. Blain, and P. Monfray (2003), An ecosystem model of the global ocean including Fe, Si, P colimitations, *Global Biogeochem. Cycles*, *17*(2), 1060, doi:10.1029/2001GB001745.

Benson, A. J., and A. W. Trites (2002), Ecological effects of regime shifts in the Bering Sea and eastern North Pacific Ocean, *Fish Fish.*, *3*, 95–113.

Bograd, S., F. Schwing, R. Mendelssohn, and P. Green-Jessen (2002), On the changing seasonality over the North Pacific, *Geophys. Res. Lett.*, *29*(9), 1333, doi:10.1029/2001GL013790.

Bond, N. A., J. E. Overland, M. Spillane, and P. Stabeno (2003), Recent shifts in the state of the North Pacific, *Geophys. Res. Lett.*, *30*(23), 2183, doi:10.1029/2003GL018597.

Boyd, P., and P. J. Harrison (1999), Phytoplankton dynamics in the NE subarctic Pacific, *Deep Sea Res., Part II*, *46*, 2405–2432.

Boyd, P. W., F. A. Whitney, and P. J. Harrison (1995), The NE subarctic Pacific in winter. 2. Biological rate processes, *Mar. Ecol. Prog. Ser.*, *128*, 25–34.

Boyd, P. W., D. L. Muggli, D. E. Varela, R. H. Goldblatt, R. Chretien, K. J. Orians, and P. J. Harrison (1996), In vitro iron enrichment experiments in the NE subarctic Pacific, *Mar. Ecol. Prog. Ser.*, *136*, 179–193.

Brickley, P. J., and A. C. Thomas (2004), Satellite-measured seasonal and interannual chlorophyll variability in the northeast Pacific and coastal Gulf of Alaska, *Deep Sea Res., Part II*, *51*, 229–245.

Brodeur, R. D., and D. M. Ware (1992), Long-term variability in zooplankton biomass in the subarctic Pacific Ocean, *Fish. Oceanogr.*, *1*, 32–38.

Brodeur, R. D., B. W. Frost, S. R. Hare, R. C. Francis, and W. J. Ingraham (1996), Interannual variations in zooplankton biomass in the Gulf of Alaska and covariation with California Current zooplankton biomass, *CalCOFI Rep. 37*, pp. 80–99, Calif. Coop. Oceanic Fish. Invest., La Jolla.

Capotondi, A., M. A. Alexander, C. Deser, and A. J. Miller (2005), Low frequency pycnocline variability in the northeast Pacific, *J. Phys. Oceanogr.*, *35*, 1403–1420.

Chai, F., R. T. Barber, and S. T. Lindley (1996), Origin and maintenance of high nutrient condition in the equatorial Pacific, *Deep Sea Res., Part II*, *42*, 1031–1064.

Chai, F., R. C. Dugdale, T.-H. Peng, F. P. Wilkerson, and R. T. Barber (2002), One-dimensional ecosystem model of the equatorial Pacific upwelling system: part I. Model development and silicon and nitrogen cycle, *Deep Sea Res., Part II*, *49*, 2713–2745.

Chai, F., M. Jiang, R. T. Barber, R. C. Dugdale, and Y. Chao (2003), Interdecadal variation of the transition zone chlorophyll front: A physical-biological model simulation between 1960 and 1990, *J. Oceanogr.*, *59*, 461–475.

Chai, F., M.-S. Jiang, Y. Chao, R. C. Dugdale, F. Chavez, and R. T. Barber (2007), Modeling responses of diatom productivity and biogenic silica export to iron enrichment in the equatorial Pacific Ocean, *Global Biogeochem. Cycles*, *21*, GB3S90, doi:10.1029/2006GB002804.

Coale, K. H., et al. (1996), A massive phytoplankton bloom induced by an ecosystem-scale iron fertilization experiment in the equatorial Pacific Ocean, *Nature*, *838*, 495–501.

Cummins, P. F., and G. S. Lagerloef (2002), Low frequency pycnocline depth variability at station P in the northeast Pacific, *J. Phys. Oceanogr.*, *32*, 3207–3215.

da Silva, A. M., C. C. Young-Molling, and S. Levitus (Eds.) (1994), *Atlas of Surface Marine Data 1994*, vol. 1, *Algorithms and Procedures*, *NOAA Atlas NESDIS*, vol. 6, 83 pp., NOAA, Silver Spring, Md.

de Boyer Montégut, C., G. Madec, A. S. Fischer, A. Lazar, and D. Iudicone (2004), Mixed layer depth over the global ocean: An examination of profile data and a profile-based climatology, *J. Geophys. Res.*, *109*, C12003, doi:10.1029/2004JC002378.

Deser, C., M. A. Alexander, and M. S. Timlin (1996), Upper ocean thermal variations in the North Pacific during 1970–1991, *J. Clim.*, *9*, 1841–1855.

Deser, C., M. A. Alexander, and M. S. Timlin (1999), Evidence for wind-driven intensification of the Kuroshio Current Extension from the 1970s to the 1980s, *J. Clim.*, *12*, 1697–1706.

Deser, C., A. S. Phillips, and J. W. Hurrell (2004), Pacific interdecadal climate variability: Linkages between the tropics and the North Pacific during boreal winter since 1900, *J. Clim.*, *17*, 3109–3124.

Evans, T. G., and J. S. Parslow (1985), A model of annual plankton cycles, *Biol. Oceanogr.*, *3*, 327–347.

Fasham, M. J. R. (1995), Variations in the seasonal cycle of biological production in subarctic oceans: A model sensitivity analysis, *Deep Sea Res., Part I*, *42*, 1111–1149.

Francis, R. C., S. R. Hare, A. B. Hollowed, and W. S. Wooster (1998), Effects of interdecadal climate variability on the oceanic ecosystems of the NE Pacific, *Fish. Oceanogr.*, *7*, 1–21.

Freeland, H., K. Denman, C. S. Wong, F. Whitney, and R. Jacques (1997), Evidence of change in the winter mixed layer in the northeast Pacific Ocean, *Deep Sea Res., Part I*, *44*, 2117–2129.

Frost, B. W. (1991), The role of grazing in nutrient-rich areas of the open sea, *Limnol. Oceanogr.*, *36*, 1616–1630.

Frost, B. W., and N. C. Frazen (1992), Grazing and iron limitation in the phytoplankton stock and nutrient concentration: A chemostat analogue of the Pacific equatorial upwelling zone, *Mar. Ecol. Prog. Ser.*, *83*, 291–303.

Fung, I. Y., S. K. Meyn, I. Tegen, S. C. Doney, J. G. John, and J. K. B. Bishop (2000), Iron supply and demand in the upper ocean, *Global Biogeochem. Cycles*, *14*, 281–295.

Gargett, A. E. (1997), The optimal stability 'window': A mechanism underlying decadal fluctuations in North Pacific salmon stocks?, *Fish. Oceanogr.*, *6*, 109–117.

Gent, P. R., and J. C. McWilliams (1990), Isopycnal mixing in ocean circulation models, *J. Phys. Oceanogr.*, *20*, 150–155.

Gent, P. R., F. O. Bryan, G. Danabasoglu, S. Doney, W. R. Holland, W. G. Large, and J. C. McWilliams (1998), The NCAR climate system model global ocean component, *J. Clim.*, *11*, 1287–1306.

Graham, N. E. (1994), Decadal-scale climate variability in the tropical and North Pacific during the 1970s and 1980s: Observations and model results, *Clim. Dyn.*, *6*, 135–162.

Gregg, W. W. (2002), Tracking the SeaWiFS record with a coupled physical/biogeochemical/radiative model of the global oceans, *Deep Sea Res., Part II*, *49*, 81–105.

Gregg, W. W., P. Ginoux, P. S. Schopf, and N. W. Casey (2003), Phytoplankton and iron: Validation of a global three-dimensional ocean biogeochemical model, *Deep Sea Res., Part II*, *50*, 3143–3169.

Haigh, S. P., K. L. Denman, and W. W. Hsieh (2001), Simulation of the planktonic ecosystem response to pre- and post-1976 forcing in an isopycnic model of the North Pacific, *Can. J. Fish. Aquat. Sci.*, *58*, 703–722.

Hare, S. R., and N. J. Mantua (2000), Empirical evidence for North Pacific regime shifts in 1977 and 1989, *Prog. Oceanogr.*, *47*, 103–145.

Harrison, P. J. (2006), SERIES (subarctic ecosystem response to iron enrichment study): A Canadian-Japanese contribution to our understanding of the iron-ocean-climate connection, *Deep Sea Res., Part II*, *53*, 2006–2011.

Johnson, K. S., R. M. Gordon, and K. H. Coale (1997), What controls dissolved iron concentrations in the world ocean?, *Mar. Chem.*, *57*, 137–161.

Johnson, K. S., J. K. Moore, and W. O. Smith (2002), Workshop highlights iron dynamics in ocean carbon cycle, *Eos Trans. AGU*, *83*(43), 482.

Kalnay, E., et al. (1996), The NCEP/NCAR 40-year reanalysis project, *Bull. Am. Meteorol. Soc.*, *77*, 437–471.

Kistler, R., et al. (2001), The NCEP-NCAR 50-year reanalysis: Monthly means CD-ROM and documentation, *Bull. Am. Meteorol. Soc.*, *82*, 247–267.

Lagerloef, G. (1995), Interdecadal variations in the Alaska Gyre, *J. Phys. Oceanogr.*, *25*, 2242–2258.

Landry, M. R., et al. (1997), Iron and grazing constraints on primary production in the central equatorial Pacific: An EQPAC synthesis, *Limnol. Oceanogr.*, *42*, 405–418.

Large, W. C., J. C. McWilliams, and S. C. Doney (1994), Oceanic vertical mixing: A review and a model with a nonlocal boundary layer parameterization, *Rev. Geophys.*, *32*, 363–404.

Large, W. G., G. Danabasoglu, S. C. Doney, and J. C. McWilliams (1997), Sensitivity to surface forcing and boundary layer mixing in a global ocean model: Annual mean climatology, *J. Phys. Oceanogr.*, *27*, 2418–2447.

Levitus, S., R. Burgett, and T. P. Boyer (1994), *World Ocean Atlas 1994*, vol. 3, *Salinity, NOAA Atlas NESDIS*, vol. 3, 111 pp., NOAA, Silver Spring, Md, 1994.

Li, M., P. G. Myers, and H. Freeland (2005), An examination of historical mixed layer depths along line P in the Gulf of Alaska, *Geophys. Res. Lett.*, *32*, L05613, doi:10.1029/2004GL021911.

Li, X., Y. Chao, J. C. McWilliams, and L.-L. Fu (2001), A comparison of two vertical-mixing schemes in a Pacific Ocean general circulation model, *J. Phys. Oceanogr.*, *14*, 1377–1398.

Mackas, D. L., R. Goldblatt, and A. G. Lewis (1998), Interdecadal variation in developmental timing of Neocalanus plumchrus populations at ocean station P in the subarcic Pacific, *Can. J. Fish. Aquat. Sci.*, *55*, 1878–1893.

Maldonado, M. T., P. T. Boyd, P. J. Harrison, and N. P. Price (1999), Co-limitation of phytoplankton by light and Fe during winter in the subarctic Pacific Ocean, *Deep Sea Res., Part II*, *46*, 2475–2485.

Mann, K. H. (1993), Physical oceanography, food chains, and fish stocks: A review, *ICES J. Mar. Sci.*, *50*, 105–119.

Mantua, N. J., S. R. Hare, Y. Zhang, J. M. Wallace, and R. C. Francis (1997), A Pacific interdecadal climate oscillation with impacts on salmon production, *Bull. Am. Meteorol. Soc.*, *78*, 1069–1079.

Martin, J. H., and S. E. Fitzwater (1988), Iron deficiency limits phytoplankton growth in the northeast Pacific subarctic, *Nature*, *331*, 341–343.

McClain, C. R., K. Arrigo, K.-S. Tai, and D. Turk (1996), Observations and simulations of physical and biological processes at ocean weather station P, 1951–1980, *J. Geophys. Res.*, *101*, 3697–3713.

McFarlane, G. A., and R. J. Beamish (1992), Climatic influence linking copepod production with strong year-class in sablefish, Anoplopoma fimbria, *Can. J. Fish. Aquat. Sci.*, *49*, 743–753.

Miller, A. J., D. R. Cayan, T. P. Barnett, N. E. Graham, and J. M. Oberhuber (1994), Interdecadal variability of the Pacific Ocean: Model response to observed heat flux and wind stress anomalies, *Clim. Dyn.*, *10*, 287–302.

Miller, A. J., F. Chai, S. Chiba, J. R. Moisan, and D. J. Neilson (2004), Decadal-scale climate and ecosystem interactions in the North Pacific Ocean, *J. Oceanogr.*, *60*, 163–188.

Moore, J. K., S. C. Doney, and K. Lindsay (2004), Upper ocean ecosystem dynamics and iron cycling in a global three-dimensional model, *Global Biogeochem. Cycles*, *18*, GB4028, doi:10.1029/2004GB002220.

Newman, M., G. P. Compo, and M. A. Alexander (2003), ENSO-forced variability of the Pacific Decadal Oscillation, *J. Clim.*, *16*, 3853–3857.

Polovina, J. J., G. T. Mitchum, N. E. Graham, M. P. Craig, E. E. DeMartini, and E. N. Flint (1994), Physical and biological consequences of a climate event in the central North Pacific, *Fish. Oceanogr.*, *3*, 15–21.

Polovina, J. J., G. Mitchum, and G. T. Evans (1995), Decadal and basin scale variation in mixed layer depth and the impact on biological production in the central and North Pacific, 1960–1988, *Deep Sea Res., Part I*, *42*, 1701–1716.

Rand, P. S., and S. G. Hinch (1998), Spatial patterns of zooplankton biomass in the northeast Pacific Ocean, *Mar. Ecol. Prog. Ser.*, *171*, 181–186.

Roden, G. I. (1964), Shallow temperature inversions in the Pacific Ocean, *J. Geophys. Res.*, *69*, 2899–2914.

Seager, R., Y. Kushnir, and M. A. Cane (1995), On heat flux boundary conditions for ocean models, *J. Phys. Oceanogr.*, *25*, 3219–3230.

Stabeno, P. J., and J. E. Overland (2001), The Bering Sea shifts towards an earlier spring transition, *Eos Trans., AGU*, *82*, 317–321.

Steele, J. H., and E. W. Henderson (1993), The significance of interannual variability, in *Towards a Model of Ocean Biogeochemical Processes*, *NATO ASI Ser.*, vol. 1, edited by G. T. Evans and M. J. R. Fasham, pp. 237–260, Springer, New York.

Sugimoto, T., and K. Tadokoro (1997), Interannual-interdecadal variations in zooplankton biomass, chlorophyll concentration and physical environment in the subarctic Pacific and Bering Sea, *Fish. Oceanogr.*, *6*, 74–93.

Trenberth, K. E. (1990), Recent observed interdecadal climate changes in the Northern Hemisphere, *Bull. Am. Meteorol. Soc.*, *71*, 988–993.

Trenberth, K. E., and J. W. Hurrell (1994), Decadal atmosphere-ocean variations in the Pacific, *Clim. Dyn.*, *9*, 303–319.

Venrick, E. L., J. A. McGowan, D. R. Cayan, and T. L. Hayward (1987), Climate and chlorophyll a: Long-term trends in the central North Pacific Ocean, *Science*, *238*, 70–72.

Wilks, D. S. (1995), *Statistical Methods in the Atmospheric Sciences: An Introduction*, 467 pp., Academic, New York.

Zhang, Y., J. M. Wallace, and D. S. Battisti (1997), ENSO-like interdecadal variability, *J. Clim.*, *10*, 1004–1020.

M. Alexander and A. Capotondi, Earth System Research Laboratory, Physical Science Division, NOAA, R/PSD1, 325 Broadway, Boulder, CO 80305-3328, USA. (michael.alexander@noaa.gov)

R. Brodeur, Northwest Fisheries Science Center, Hatfield Marine Science Center, Oregon State University, 2030 South Marine Science Drive, Newport, OR 97365, USA.

F. Chai, School of Marine Sciences, University of Maine, 5706 Aubert Hall, Orono, ME 04469, USA.

C. Deser, Climate and Global Dynamics Division, NCAR, 1850 Table Mesa Drive, Boulder, CO 80305, USA.

A. Miller, Scripps Institution of Oceanography, University of California, San Diego, 9500 Gilman Drive, La Jolla, CA 92093, USA.